Ind. J. Pharm. Edu. Res., 2025; 59(2s):s560-s571.
https://www.ijper.org

Original Article

Exploration of Smart Utilization of Biodegradable Nanobubbles in Intensifying the Capsaicin Bioavailability

Hema Kumar A V[1], Chamakuri Kantlam[2,*]

[1]Bharatiya Engineering Science and Technology Innovation University (BESTIU), Gownivaripalli, Gorantala Mandal, Anantapur, Andhra Pradesh, INDIA.
[2]Brilliant Grammar School Educational Society's Group of Institutions- Integrated Campus (Faculty of Engineering and Faculty of Pharmacy), Abdullapur, Abdullapurmet, Ranga Reddy, Hyderabad, Telangana, INDIA.

ABSTRACT

Background: Capsaicin (CAP), a naturally occurring alkaloid, shows many promising benefits but is unexplored due to its hydrophobic nature and limited bioavailability. **Objectives:** To address these limitations, the present study was focused on optimizing Polylactic acid co-Glycolic Acid (PLGA) nanobubbles as a sustained delivery system for capsaicin. Nanobubbles offer advantages such as enhanced solubility, stability, and bioavailability of capsaicin. **Materials and Methods:** CAP-PLGA nanobubble optimization was achieved by implementing a three-factor, three-level Box Behnken Design (BBD) and a total of 15 experimental runs, including three replicated centre points. The formulated nanobubbles were analysed and evaluated for particle size, polydispersity index, zeta potential, drug entrapment efficiency, compatibility studies *in vitro* studies, and stability studies along with *in vivo* studies in rats. **Results:** The optimized Nanobubbles (NBs) displayed a particle size of 164.07±6.4 nm, polydispersity index of 0.261±0.09 with a (ZP) Zeta Potential of -40.5±6.2 mV and Entrapment Efficiency (EE) of 81.06±3.58. *In vitro* studies revealed a superior drug release (96.8%) with ultrasound versus plain drugs (28%). Fourier transform infrared spectroscopy; differential scanning calorimetry and X-ray diffraction studies confirmed no drug-polymer interaction. Scanning Electron Microscopy (SEM) images showcased uniform spherical nano-sized particles. Stability studies indicated no significant changes after 1 month. The nanobubbles exhibited increased C_{max} (4.47) and AUC_{0-t} (7.29), promising enhanced sustained release, absorption, and extended the half-life. **Conclusion:** The present study results indicated that CAP-loaded PLGA NBs effectively showed an impact on kinetics of the drug in sustaining its release for a prolonged period and as well as bioavailability of orally administered dose in rats. The utilization of the nanobubble formulation potentially improved the bioavailability of capsaicin in the human body. Targeted medicine delivery is made possible by a potential use of nanobubbles in the creation of ultrasonic-responsive combinations.

Keywords: Box-Behnken design, Capsaicin, Nanobubbles, PLGA.

Correspondence:
Dr. Chamakuri Kantlam
Professor and Principal, Brilliant Grammar School Educational Society's Group of Institutions- Integrated Campus (Faculty of Engineering and Faculty of Pharmacy), Abdullapur, Abdullapurmet, Ranga Reddy, Hyderabad-501505, Telangana, INDIA.
Email: kantlam22@gmail.com

Received: 09-05-2024;
Revised: 29-08-2024;
Accepted: 26-12-2024.

INTRODUCTION

Capsaicin (CAP), a naturally occurring alkaloid present in chili peppers, is renowned for its strong and spicy flavor. Apart from capsaicin, the capsaicinoid group primarily includes dihydrocapsaicin, non-dihydrocapsaicin, homohydrocapsaicin, homodihydrocapsaicin, and nonivamide.[1] It has garnered a considerable attention due to its numerous pharmacological properties and potential therapeutic uses. Research has shown that capsaicin possesses anti-inflammatory, analgesic, antioxidant, and anticancer properties. Furthermore, it has been investigated for its potential role in weight management, cardiovascular health, and neuroprotection. Capsaicin acts by interacting with sensory neurons, specifically targeting the TRPV1 receptor (Transient Receptor Potential Vanilloid 1), which is involved in pain sensation and temperature control.[2] When capsaicin activates the TRPV1 receptor, it triggers the release of neurotransmitters like substance P, resulting in pain relief and other physiological responses.[3] Additionally, capsaicin induced an apoptosis in cancer cells, making it a potential candidate. In conclusion, capsaicin exhibits great potential as a versatile compound with a wide range of therapeutic applications, necessitating further research to fully understand its capabilities.

CAP exhibits potentiality in the treatment of Alcoholic Hepatitis (AH) because of its anti-inflammatory, antioxidant, and liver-regenerating qualities. Nevertheless, additional studies, such as clinical trials, are required to validate its effectiveness and safety in treating AH.[4]

DOI: 10.5530/ijper.20257237

Despite the potential advantages, capsaicin has not been extensively studied due to various limitations. These limitations include low oral bioavailability, hydrophobicity, and adverse gastrointestinal effects such as gastric irritation, burning diarrhoea, nausea, and vomiting.[5] Consequently, there is an urgent requirement to devise a formulation strategy that can address these challenges and improve the oral bioavailability of capsaicin.

Mayuri *et al*., recently developed capsaicin-loaded micelles for active hepatic targeting using CS-g-Stearic Acid (SA) and GA (Glycyrrhetinic Acid)-conjugated (SA) Stearic Acid grafted chitosan polymers.[6] However, the study lacks *in vivo* validation of the formulations, which is a major limitation. The approaches face limitations due to challenges such as scalability issues, also depend on expensive specialized excipients, and it's a time-consuming synthesis process.

In addition to improve the solubility, it is crucial to have a method that can direct drug molecules to diseased tissues while minimizing their presence in healthy tissues. This targeted delivery system will not only enhance stability in bodily fluids and optimize concentration and release kinetics in the bloodstream, but also improve pharmacokinetic and pharmacodynamic properties. These combined factors play a significant role in increasing effectiveness and decreasing side effects. Smart delivery systems, particularly those aimed at cancer treatment, stand as an example of such systems.

Nanobubbles, tiny bubbles at the nanoscale, are utilized in various fields, particularly in drug delivery systems due to their exceptional physical characteristics. They offer remarkable stability, high internal pressure, and a large surface-to-volume ratio.[7] Nanobubbles, range in size from 500 nm to 1 nm. They may be customized precisely using amphiphilic polymers or surfactants, while research has been conducted on both polymeric and lipidic nanobubbles, and lipid-based nanobubbles are less stable, resulting in a short circulation period.[8]

PLGA (Polylactic co-Glycolic Acid), an exceptional nano/micro biomaterial, is extensively utilized in various fields including targeted drug delivery, molecular diagnostics, tissue engineering, and gene transfer. The widespread utility of PLGA is attributed to its remarkable properties, which include exceptional stability, biodegradability, and ease of chemical modification. Numerous researchers had recorded the use of PLGA as a polymer in the production of nanobubbles for the targeted delivery of a wide range of drugs, owing to its diverse benefits and suitability.[9] To the best of knowledge and based on available literature, there are no prior studies documented the utilization of PLGA Nanobubbles (NBs) for delivering capsaicin.

This research addressed a void in the field by utilizing PLGA Nanobubbles (NBs) for capsaicin delivery, implemented a Design of Experiments (DoE) for enhancement. DoE simplified the process of optimizing experimental variables through clear-cut strategies and statistical methods. The study involved the preparation of capsaicin-loaded NBs using PLGA, followed by comprehensive *in vitro* and *in vivo* evaluation.

MATERIALS AND METHODS

Reagents and chemicals

Capsaicin was purchased from AOS Products Pvt. Ltd., Ghaziabad. C3F8 (Perfluoro propane) was procured from Pharm affiliates Pvt. Ltd., Haryana, India. Sigma Aldrich, US, supplied Poly (D, L-lactide-co-glycolide) 50:50 with an intrinsic viscosity of 0.22 dL/g and Mw 25,000. Polyvinyl Alcohol (PVA; Mw 30,000-70,000) was purchased from Sigma Aldrich (St. Louis, MO, USA). Isopropanol, and dichloromethane was acquired from S.D. fine chemicals, Hyderabad. Acetonitrile was purchased from Qualigens, India.

Analytical method development using RP-HPLC

Chromatographic analysis of capsaicin was executed using RP-HPLC technique, employing a Develosil ODS HG-5 RP C18 column (150x4.6 mm, 5 µm). The mobile phase included a blend of methanol and double distilled water in a 60:40 (v/v) ratio. The flow was set to 1.0 mL/min. Detection was carried out at 280 nm. A standard stock solution of capsaicin at a concentration of 1000 µg/mL was prepared, followed by a creation of various working standard solutions ranging from 0.5 to 100 µg/mL through serial dilutions. A stock solution (1000 µg/mL)of dihydrocapsaicinas IS (Internal Standard) after appropriate dilution was included in the experiment.[10]

Capsaicin Nanobubbles (CAP-NBs) formulation development and optimization

Capsaicin-loaded PLGA nanobubbles were synthesized using a solvent evaporation method with ultrasound assistance following a modified protocol.[11] At first, a homogeneous solution was formed by dissolving PLGA in a water-immiscible solvent, namely Dichloromethane (DCM). The drug (CAP) was then added to create a dispersion, which underwent sonication for 2 min at 45% amplitude in an ice bath using a Digital Sonifier S-250D (Branson Ultrasonic, Danbury, USA). Next, the drug dispersion was combined with 20 mL of chilled 2.0% PVA (Polyvinyl Alcohol) solution and homogenized at 6,500 rpm for 10 min using a high-speed homogenizer. This was followed by sonication at 30 W for 1 min in the absence of light using an ultrasonic probe. To eliminate the dichloromethane, a 2.5% v/v isopropanol solution (20 mL) was added to the emulsion and mechanically stirred for 5 hr. After that, the resulting product was centrifuged for 5 min at 8000 rpm. The formed precipitate was washed with distilled water after discarding the supernatant. This centrifugation and washing process was repeated three times. The nanobubbles were subsequently freeze-dried in the absence of light for 36 hr using a LYPH LOCK 4.5 (Labconco Corporation, kansascity). Later,

Table 1: Factors influencing the experiments design (Drug amount is 30 mg).

	Variables	Levels		
		LOW (-1)	Medium (0)	High (+1)
A	Stabilizer Concentration (w/v).	0. 5	1.50	2.0
B	Homogenization Speed (HS, rpm).	10000.00	12000.00	15000.00
C	Homogenization Duration (HD, min).	5	7.50	10
Replies		Restrictions		
X	Particle Size (PS)	Minimize		
Y	Polydispersity Index (PdI).	Minimize		
Z	Entrapment Efficiency percentage (EE%).	Maximum		

C3F8 gas (perfluoropropane) was added to the lyophilization chamber through a vial connector at a flow level of 50 mL/min for 1 min. After this, the screw vials were tightly sealed for further analysis. CAP loaded PLG Ananobubble optimization was achieved by implementing a three-factor, three-level BBD. A total of 15 experimental runs, including three replicated centre points, comprised the Box-Behnken Design (BBD)[12]. Three independent variables were stabilizer concentration, homogenization speed, and homogenization duration varied at low (-1), middle (0), and high (1) levels. The drug-to-PLGA ratio was consistently maintained at 0.1:1 (w/w). The measured variables included particle size (Y1), polydispersity index (Y2), and Encapsulation Efficiency (EE%) (Y3). Table 1 listed their respective ranges. Utilizing Response Surface Charts and contour (2D) plots, response surface search was carried out with Design Expert® tools (Edition 12, Stat-Ease Inc., Minneapolis, MN).

Characterisation and Evaluation

Measurements of Particle Size (PS) of nanobubbles

The PS, PdI (Polydispersity Index) and ZP of CAP-NBs were determined after a tenfold dilution of the sample with double-distilled water using a Malvern Zetasizer with the application of DLS (Dynamic Light Scattering) theory.[9]

Entrapment Efficiency (EE) and Load Capacity (LC)

EE and LC assessment included dissolving a specific quantity of drug-loaded Nanobubbles (NBs) in dichloromethane, followed by sonication for 12 min to dissolve the complex. The solution obtained was then appropriately diluted and analyzed employing a UV-Vis spectrophotometer at 282 nm. The following formulas were used calculate EE and LC.[13]

$$\%\ Encapsulation\ efficiency(EE) = \frac{Total\ amount\ of\ the\ drug - free\ drug}{Total\ amount\ of\ drug} \times 100$$

$$\%\ Loading\ capacity(LC) = \frac{Total\ amount\ of\ the\ drug - free\ drug}{Weight\ of\ the\ nanobubble\ formulation\ taken} \times 100$$

Fourier Transform Infrared Spectroscopy study (FTIR)

The spectra analysis involved studying Capsaicin (CAP), a physical blend of PLG A and PVA, and an optimized Nanobubbles (NBs). The KBr disc method was used for this analysis with a Tensor 27 FTIR spectrophotometer, examining a spectral range from 4000 to 500 cm^{-1}.[14]

Differential Scanning Calorimeter (DSC)

The thermal behavior of the samples (2 mg) was analyzed using DSC (Mettler Toledo DSC-1). The specimens were heated at a rate of 10°C per min while being contained in aluminum pans, ranging from 20 to 400°C.[15]

Scanning Electron Microscopy (SEM)

With the Quanta FESEM 250 SEM, images of the drug and NBs' structure were captured. Prior to analysis, the sample underwent sputter coating with Au via an ion sputter and was then affixed to double-sided adhesive carbon tape before being mounted on aluminium pin stubs. The specimens were analyzed from a distance of 10 mm, with magnification ranging from 500 to 10,000 times, and utilizing a 30 kV accelerating voltage.[13]

X-ray Diffraction pattern (XRD)

The Capsaicin (CAP), PLGA+PVA mixture, PLGA, and the optimized Nanobubbles (NBs) were analyzed by X-ray diffractometer (Philips; PW-1710). The diffraction patterns of X-rays were generated using a monochromator (graphite) and Ni-filtered Cu Kα radiation. Copper (Cu Kα) radiation was used for XRD investigation at 40 kV and 30 mA. The samples were scanned between 2 and 80° 2 theta (θ) with an average step size of 0.045° and a duration per step of 0.5 sec.[16]

Drug Release (DR)

The cumulative DR of CAP from the nanobubbles was assessed at 37±0.5°C using both the dialysis bag method with and without ultrasonography. Nanobubbles containing 10 mg of CAP were sited in dialysis membrane bag and submerged in 100 mL of pH 7.4 phosphate buffer as the release medium. The system was

agitated at 300 revolutions per minute (rpm), and 5 mL samples were collected at designated time intervals. An equivalent volume media was added in order to continue sink environment. The amount of CAP in the media was measured at 282 nm by UV-visible spectroscopy, and the cumulative release percentage of CAP was computed.[17]

Stability of CAP-loaded NBs

The stability of CAP-loaded NBs was evaluated over three months at various temperatures as per literature. PS, PdI and EE were measured on days 1, 30, 45, 60, and 90 to assess stability.[18]

Pharmacokinetic studies

Male Wistar rats, weighing around 200±20 g and aged between 4 and 5 weeks, were obtained from the ICMR-NIN institute for research, Telangana. The animal study was approved by the Institutional Animal Ethics Committee (IAEC) with the protocol number 1447/PO/Re/S/11/CPCSEA-84/A. The rats were allowed to acclimate for seven days at a temperature of 20°C±2. The animals were split into two sorts, each consisting of six animals. The Nanobubble (NBs) formulation (2 mg/kg BW) and Capsaicin (CAP) dispersed in 0.25% w/v sodium carboxymethylcellulose were administered p.o. Blood samples of 250 µL were accrued from the retroorbital plexus at predetermined intervals and centrifuged at 7500 rpm for 10 min using a cooling centrifuge (Effendorf). The extracted plasma was analysed using HPLC.[19]

Method for Preparing Samples and Bioanalytical Method Establishment

Protein precipitation was used to remove CAP from the blood samples. In summary, approximately 250 mL of acetonitrile was used to quench 50 µL of rat plasma containing dihydrocapsaicinas, which served as an internal standard. The mixture sample was vortexed and centrifuged for 12 min at 8,000 rpm. RP-HPLC was used to separate and examine the supernatant. The HPLC method described previously in the analytical part was used for bio-analysis.

Data and statistical study

WinNonlin (version 3.1; Pharsight Co., Mountain View, CA, USA) was used to evaluate the *in vivo* data. The pharmacokinetic variables were examined using the non-compartmental technique. The Mean±Standard Deviation (SD) represented the pharmacokinetic variables. Additionally, GraphPad Prism (GraphPad Software 8.05 Inc., CA) was utilized as a statistical analysis program to further investigate the variables.

RESULTS AND DISCUSSION

Capsaicin Nanobubbles (CAP-NBs) formulation development and optimization

The study involved a creation of capsaicin nanobubbles through the combination of the solvent evaporation method and ultrasound. PLGA dissolved in DCM was mixed with the drug, sonicated, and then added to a chilled 2.0% w/v PVA solution.

Table 2: Runs designed for the trails.

		Factor 1	Factor 2	Factor 3	Response 1	Response 2	Response 3
Run	CAP amount	A: Stabilizer concentration	B: Homogenization Speed (HS)	C: Homogenization Duration (HD)	Particle size	PdI	Entrapment Efficiency (EE)
		Ratio	Rpm	min	nm		%
1	30 mg	1.25	12500	9	199.6	0.223	64.44
2		1.25	10000	6	200.36	0.381	72.24
3		1.25	10000	12	186.9	0.331	71.74
4		2	10000	9	216	0.362	63.28
5		1.25	12500	9	214.2	0.293	65.9
6		0.5	10000	9	164	0.142	80.98
7		1.25	12500	9	202.8	0.351	69.32
8		0.5	15000	9	203.8	0.289	54.87
9		2	15000	9	246.2	0.318	88.68
10		2	12500	12	225.16	0.299	82.22
11		1.25	15000	6	220.81	0.375	62.02
12		2	12500	6	216.84	0.392	72.9
13		1.25	15000	12	228.22	0.364	83.44
14		0.5	12500	12	180.6	0.198	70.41
15		0.5	12500	6	182.3	0.229	68.28

Following this, high-speed homogenization and 1 min sonication at 30 W were carried out. Dichloromethane extraction was performed using a 2.5% v/v isopropanol solution while stirring at room temperature for 5 hr. The term "nanobubbles" was used instead of "nanodroplets" due to the fluidity of perfluoropentane at room temperature. Ultrasound caused a liquid-to-vapor phase transition, known as acoustic droplet vaporization, which transformed nanodroplets into nanobubbles, improving their echogenic properties in ultrasonography images.[20] The term "ultrasound" referred to pressure waves with compressional and rarefactional fluctuations at frequencies ≥20 kHz, leading to effects such as cavitation for bubble size reduction and sonoporation, which helps in the uptake of the reduced bubble.[21] Electron microscopy was utilized to directly visualize the nanobubbles and evaluate their integrity and gas composition. A combination of ultrasound along with nanobubbles helps in drug localization while overcoming the off target adverse effects.[22] PLGA was highly recommended in various medical applications including sutures, bone implants, and in sustained drug release systems due to its biocompatibility and biodegradability properties.

QbD emphasizes the precise monitoring of Critical Quality Attributes (CQAs) to achieve and maintain QTPP.[23] NBs aimed to enhance drug stability, bioavailability, and targeted delivery, addressing solubility and short half-life issues. In the current study, PS, PdI, and EE were selected as CQAs. Table 2 succinctly summarized the chosen CQAs and their rationale behind. Multiple linear regression analysis (2FI) constructed polynomial models (quadratic, two-factor, and linear). The model selection used R^2, predicted R^2, adjusted R^2, and Coefficient of Variance (C.V). ANOVA assessed variable impact on responses.

PS

The small size of NBs resulted in a significantly higher surface area-to-volume ratio, enhancing their stability, penetrability, and reactivity in targeted drug delivery.[24] After 15 trials, particle size is ranging from 164.0 to 246.2 nm. The model's F value was 46.20, with a 0.01% noise, confirmed its 'linear' nature and significant lack of fit. The variables with p-values below 0.0500 significantly impacted the response. The “lack of fit F-Value” (0.67) implied that any lack of fit, was not statistically considerable. There was 72.62% chance that a “Lack of Fit F-value” of this extent would occur due to random noise, underscoring the model’s reliability. The surface and contour plots illustrated variable influences on Particle Size (PS) and were depicted in the Figure 1. The R^2, corrected R^2 and anticipated R^2 (0.9265, 0.9064, and 0.8609) respectively showed a model precision of 22.58, surpassing the required value of 4.

Stabilizer concentration was the most influential factor affecting particle size, demonstrated that alterations in this factor result in a corresponding change in particle size. Homogenization speed, denoted by variable B, also played a role in particle size, although to a lesser extent than stabilizer concentration. Both variables A and B had a significant impact on the results, as evidenced by their p-values below 0.05. Variable C, on the other hand, had a smallest effect on particle size compared to the variables A and B. They are now considered a meaningful, and the regression equation was as followed below:

$$\text{Particle size} = 205.85 + 21.69\,A + 16.47B + 0.0712C$$

PdI

The Polydispersity Index (PdI) is a dimensionless metric that quantifies the broadness of the particle size distribution.[25] Typically, it falls between 0 and 1. Formulations exhibited PdIs

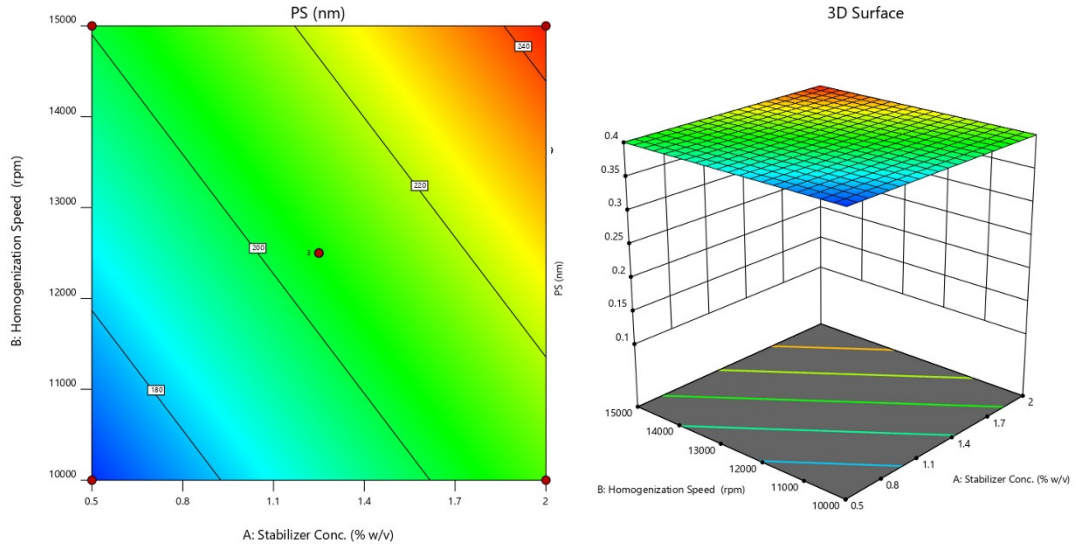

Figure 1: Response surface and contour plots illustrated variable effects on Particle Size (PS).

from 0.142 to 0.392, with a model F value of 4.07, indicated a significance of the proposed "quadratic" model and an insignificant lack of fit (F-value 0.10). There was 95.22% chance that a "Lack of Fit F-value" of this magnitude would arise due to a random noise, underscoring the model's reliability. Regression coefficients (R^2, adjusted R^2, and anticipated R^2) were 0.8800, 0.6639, and 0.5126, correspondingly, showed model's usefulness with precision exceeding the necessary value (6.834). Model terms (A) had *p*-values<0.050, signifying a substantial impact. The resulting regression equation is:

$$PDI = 0.2890 + 0.0641A + 0.0162B - 0.0231C0.3550AB - 1.13AC - 0.0477AB - 0.0155AC + 0.0097BC - 0.0472\ A^2 + 0.0360\ B^2 + 0.0377\ C^2$$

Positive coefficients signified a rise in the associated variable(s), which increased PdI, while negative coefficients indicated a decline, which reduced PdI. All formulations maintained PdI within the acceptable bounds, consistently below 0.3. The graphical image of response surface and contour plots illustrated

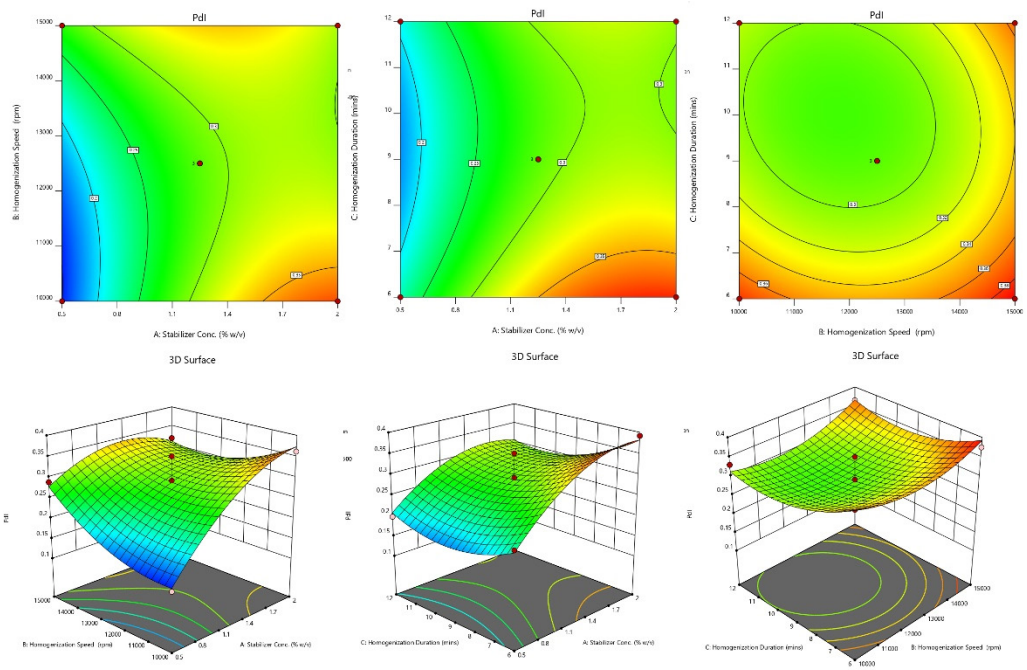

Figure 2: Graphical depiction of response surface and contour plots illustrated variable effects on Polydispersity Index (PdI).

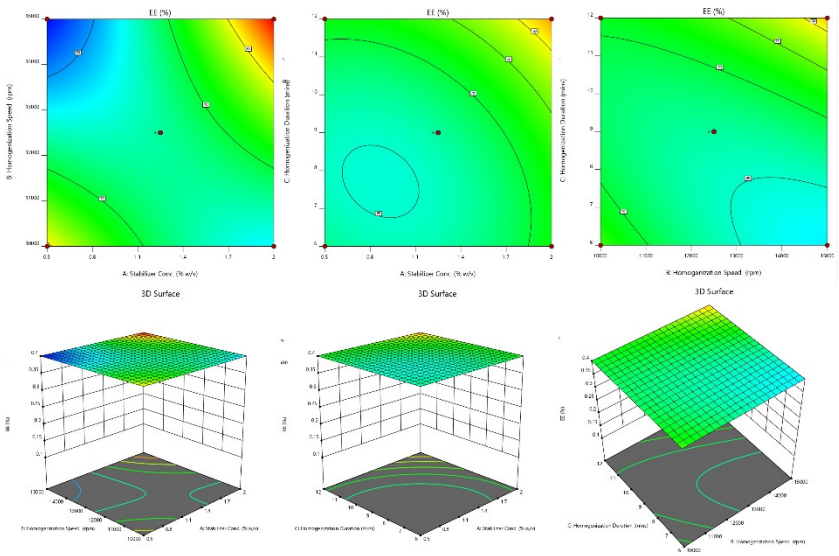

Figure 3: Graphical representation of 3 D surface and Contour Plots (CP) demonstrated its consequence of variables on EE.

variable effects on Polydispersity Index (PdI), was shown in Figure 2.

Entrapment Efficiency (EE)

Impact on EE ranged from 54.82 to 88.68%. The NBs with high entrapment was always desirable to reduce the dose of the drug.[26] The model's F value of 26.26, with a 0.11% chance was likely due to noise, indicated significance and negligible fit error for the suggested "quadratic" model. The lack of fit's F-value (0.63) was not statistically significant based on pure error, with a 66.21% probability of being noise. ANOVA identified a significant factor (p-value<0.1), leading to removal of non-significant variables. Figure 3 illustrated the contour plots and 3d response surface, which showcased the influence of selected variables on EE. The regression coefficients, R^2, adjusted R^2, and anticipated R^2, were 0.9793, 0.9420, and 0.8152, correspondingly. Predicted R^2 aligned close to an adequate R^2, differed by 0.2. The model, evidenced by adequate precision (signal-to-noise ratio) of 18.80, surpassing the necessary value of 4, proved useful for exploring the design space. An elevation in factor A (stabilizer concentration) typically resulted in enhanced entrapment efficiency, whereas elevations in factors B or C (homogenization speed and duration) had a tendency to reduce the efficiency. Moreover, interplay between factors, such as AB, and squared terms like A^2 and C^2 can exert additional influence on entrapment efficiency. By comprehending the impact of these factors on entrapment, researchers can fine-tune formulations to attain desired levels of efficiency, thereby guaranteeing the effective delivery of substances in pharmaceutical or other applications. Model terms (A, C, AB, BC, A^2, and C^2) had p-values<0.0500, that showed a significant effect. The resulting regression equation is:

$$\text{Entrapment efficiency (EE)} = +66.55 + 4.07A - 0.0962B + 4.05C + 12.88AB + 1.80AC + 5.48BC - 0.0375BC + 3.25A^2 + 2.15B^2 + 3.65C^2$$

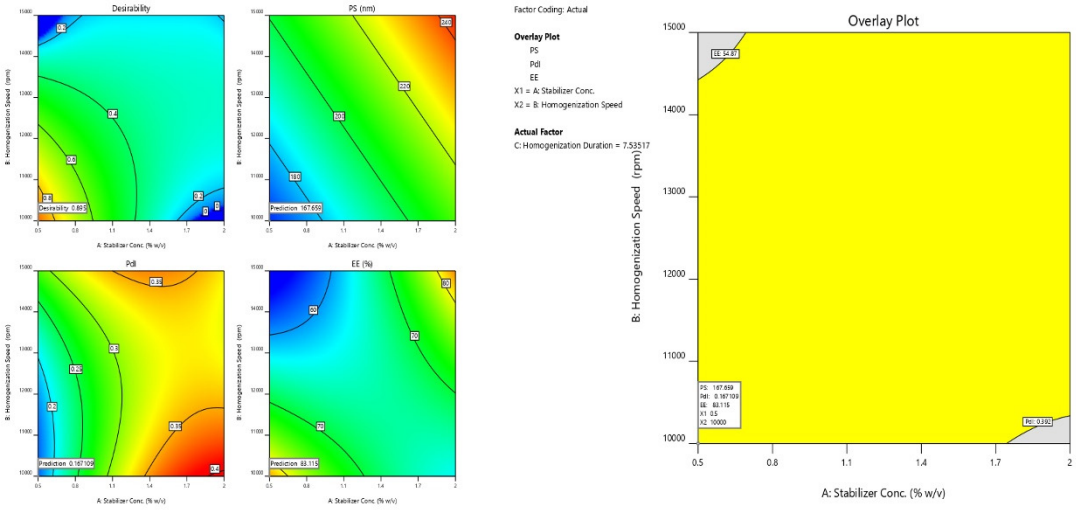

Figure 4: Graphical illustration of desirability and Overlay plot (yellow area denoted the feasible region).

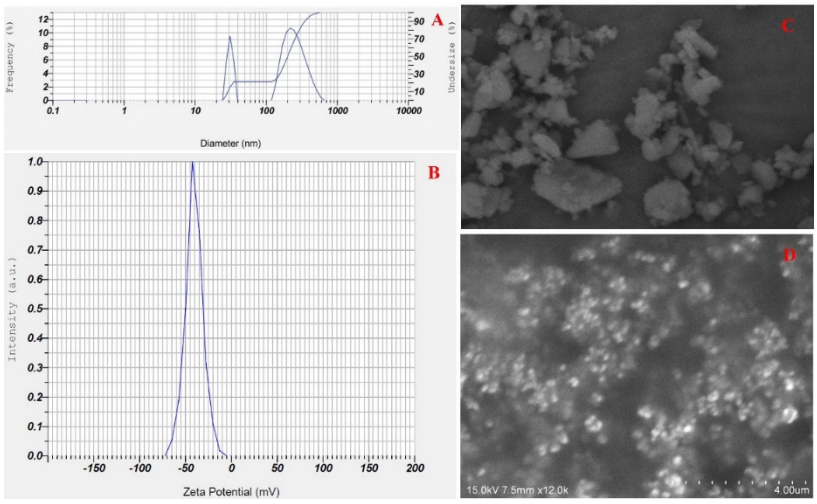

Figure 5: Malvern image of A) Particle size and PdI; B) ZP; C) SEM image of pure drug; D) CAP-PLGA Nanobubbles (NBs).

Exploration for optimized preparation

The Derringers desirability technique was utilized to optimize the variables affecting response parameters. This involved transforming response into a desirability scale, amalgamating them into a geometric mean function through exhaustive searches, ultimately yielding a global desirability value. The optimum configuration (Fopt solution) with CAP is 30 mg, stabilizer (PVA) at 0.5%w/v with a homogenization speed at 10000 and homogenization duration of 7.5 resulted in a D value of 0.895. Further graphical customization was made possible by restricting down the level of Critical Quality Attributes (CQAs), specifically low PS, PdI, and high EE.[27] Figure 4 presented the design space and overlay plot. Throughout the validation process, three checkpoints were employed to confirm the model's strength and formulation. The anticipated average size standards were 167.79 nm with a PdI of 0.167 and EE of 83.10, whereas the actual average measurements were 164±6.4 nm, PdI of 0.261±0.09, and EE of 81.06±3.58.

Characterization and evaluation of Nanobubbles (NBS)

Measurements of PS, PdI, Zeta Potential (ZP), and Loading Capacity (LC)

Particle sizes and uniformity in the formulation remained consistent, with P.S. and PdI ranging from 164±6.4 nm, and 0.261±0.09. A polydispersity value below 0.3 indicated homogeneity. The optimized formulation's Zeta potential, indicative of colloidal particle surface properties, was -40.5±6.2

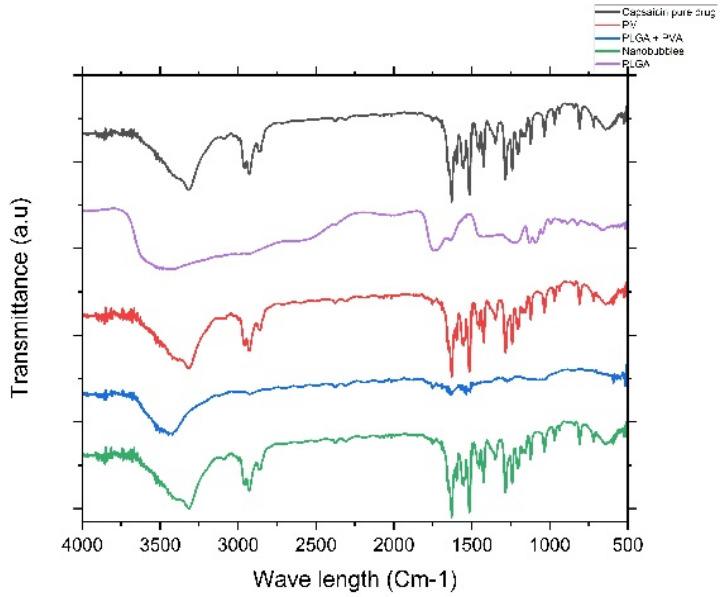

Figure 6: A) Overlay of FTIR analysis PD (black line-IBR; PM (red line-Physical mixture; IBR NBs (Blue line-Nanobubble (NS).

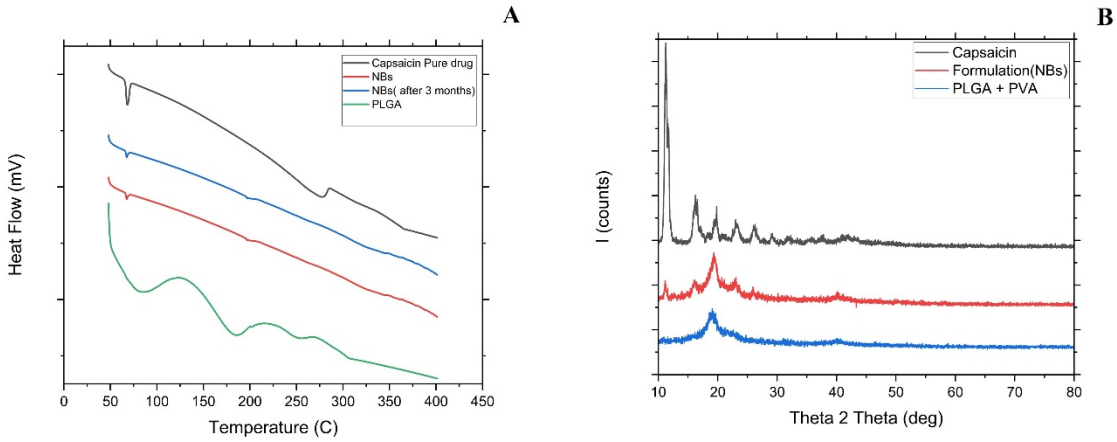

Figure 7: A) Overlay of DSC analysis Capsaicin (black line-CAP; NBs (red line-Nanobubbles; NBs (3 months- blue line); PLGA-(green line); B) Overlay of DSC analysis Capsaicin (black line- CAP; Formulation NBs (red line-Nanobubbles; PLGA+PVA-(blue line).

mV, with an EE 81.06±3.58 and LC 29.40±4.01. P.S. The particle size, and ZP of the optimized nanobubbles was depicted in Figure 5. Nanobubble stability heavily relied on elevated zeta potentials, which played a crucial role in maintaining electrostatic repulsion among particles, thus preventing their aggregation. This stability is of utmost importance as it ensures the integrity of nanobubbles during storage and administration, ultimately enhanced their performance in drug delivery and medical imaging applications.[28]

Fourier Transform Infrared Spectroscopy study (FTIR)

The interaction between capsaicin and the polymers used in nanobubble formulation was investigated through FTIR analysis (Figure 6). The spectra exhibited distinct peaks for capsaicin, such as the O-H stretch at 3447 cm^{-1}, C=O stretch at 1633 cm^{-1}, N-H bends at 1516 cm cm^{-1} C-N bonds stretching at 1283 cm^{-1}, and out-of-plane C-H bend at 806 cm^{-1}. Comparable peaks were observed for PLGA at 3455 cm^{-1}, 2886 cm^{-1}, 1762 cm^{-1}, 1186 cm^{-1}, and 1455 cm^{-1}, which corresponded to OH end group, C-H stretch, C=O stretch, C-O stretch, and C-H bends, correspondingly, as documented in the literature.[10] The FTIR spectra of optimized formulation (NBs) showed peak characteristics of capsaicin, showed minor changes that hinted at potential hydrogen bonding, linked capsaicin's -OH groups with PLGA's C=O groups. The capsaicin encapsulated in the polymer matrix implied no chemical interaction.[6]

DSC and XRD

DSC assessment was accomplished to evaluate the thermal characteristics of capsaicin, PLGA, and the nanobubbles pre and post storage for a duration of 3 months (Figure 7). Pure capsaicin exhibited a clear endothermic peak at a temperature of 68.38ºC, signified its melting point, along with a broad peak at 277.60ºC, indicated its crystalline characteristics.[29] The thermograph of PLGA exhibited peaks at 61.8ºC and 163.17ºC. In the thermographs of the nanobubbles, two fresh peaks emerged at 66.76ºC and 190.58ºC, implied a minor shift in the melting point of capsaicin and its confinement within the polymeric structure, due to the feeble intermolecular interactions between capsaicin and the polymer.[30]

Capsaicin displayed strong diffraction peaks at 5.8º, 11.7º, 16.4º and 19.8ºC, confirmed its crystalline nature. Previous studies have also reported similar diffraction peaks for capsaicin. However, in the nanobubbles, the characteristic diffraction peaks of capsaicin got vanished, suggested formation of a novel solid-state complex.[10]

Drug Release (DR)

Figure 8 depicted dissolution profiles of plain drug and drug-loaded nanobubbles without and with acoustic assistance. Drug release from nanobubbles was significantly higher than a simple drug suspension. Notably, ultrasound assistance increased the drug release. After 8 hr, Cumulative Drug Release (CDR) was 17.63±3.34%, 47.94±4.12%, and 73.44±3.67% for plain drug, nanobubbles without acoustic, and with acoustic, respectively. By 24 hr, over 96.81±4.22% was released from nanobubbles with acoustic assistance. Drug release occurred due to collapse cavitation induced by acoustic waves, disrupting nanobubble structures and enabling rapid medication release. Acoustic waves, with meticulous control and non-invasive nature, offered an accurate drug delivery and targeting abilities. These findings confirmed that ultrasound assistance played a pivotal role in enhancing CAP-the release from the nanobubbles potentially through the cavitation effect induced by ultrasound. Ultrasound stability studies indicated the transformation of the gas core from nanodroplets to bubbles, known as acoustic droplet generation. Under the influence of ultrasound, the oscillation of bubbles triggered the shell to open, thereby aided in the release of drugs. The study aligned with previous findings on nanobubble stability under varying temperature conditions. The acoustic streaming flow generated by bubble oscillation regulated the movement of detached materials, which was influenced by both the radial excursion and the duration of the ultrasound pulse.[31,32] Regulated

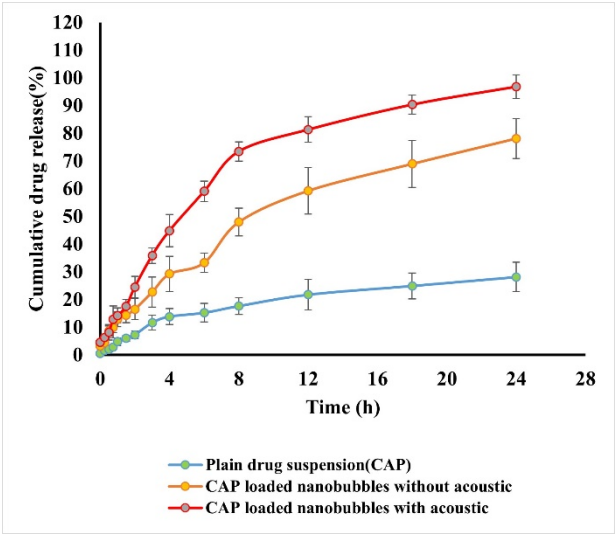

Figure 8: *In vitro* DR display in the presence and absence of ultrasound aid.

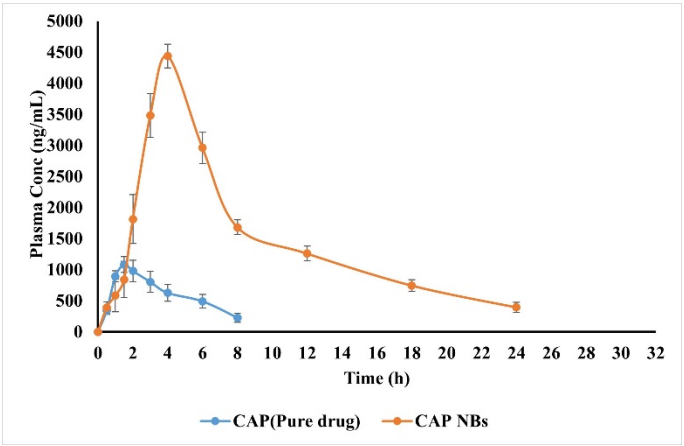

Figure 9: *In vivo* pharmacokinetic studies.

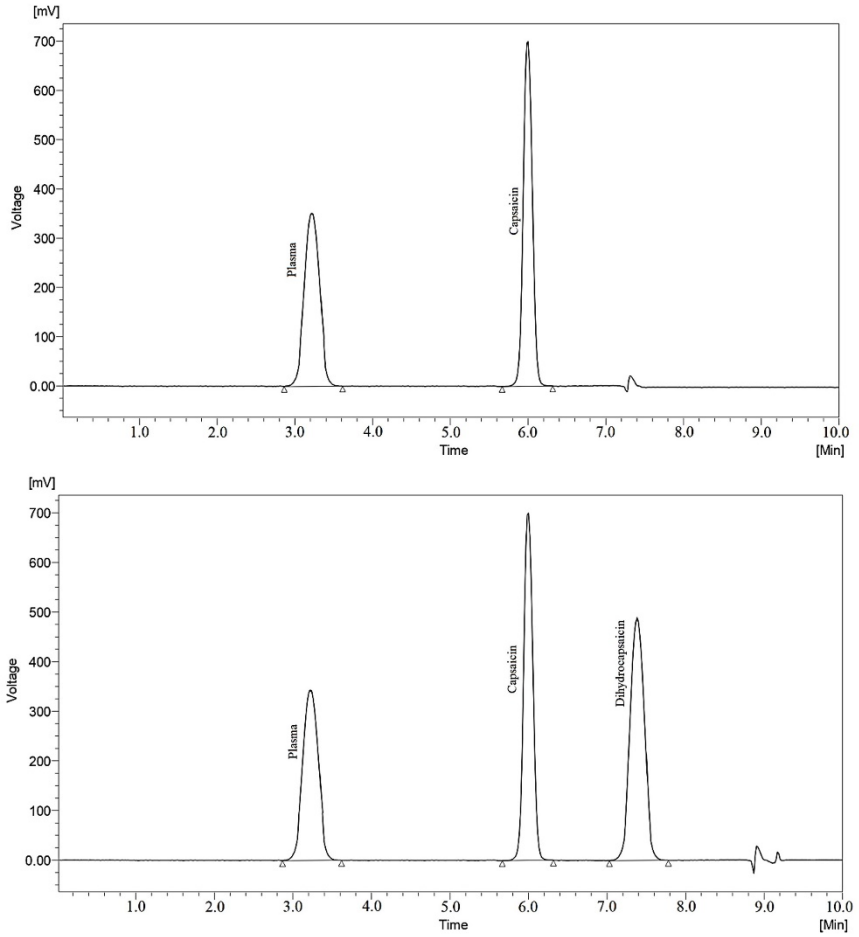

Figure 10: Bioanalytical chromatogram of drug and an internal standard in plasma that indicated drug retention time at 6.2 min and internal standard (Carbamazepine) at 7.49 min.

Table 3: Pharmacokinetic parameters of Capsaicin Pure drug and the loaded NBs.

Pharmacokinetic parameters	Capsaicin Pure drug	Capsaicin loaded NBs
C_{max} (ng/mL)	1083.02±128.98	4845.96±190.77
T_{max} (hr)	1.5	4
Half-life (hr)	3.060±0.51	7.15±1.03
AUC_{0-t} (ng. hr/mL)	4845.965±335.08	35335.145±493.48
$AUC_{0-\infty}$ (ng. hr/mL)	5846.55±362.86	39407.06±470.61
Ke (hr^{-1})	0.226	0.096
MRT (hr)	4.978±0.82	11.19±2.48

and non-invasive, acoustic waves were ideal for precise drug administration and targeting.[13]

Stability of CAP-loaded nanobubbles

CAP-loaded Nanobubbles (NBs) underwent stability assessments for 0, 1, 2, and 3 months. At 4°C and 25°C, minimal changes in drug content indicated robustness, with Encapsulation Efficiency (EE) showed a slight variation, suggested protection against degradation. However, a notable Entrapment (EE) reduction occurred at elevated temperatures where EE was reduced to 77.62±3.26% from 81.06±3.58, indicating structural disruption. Throughout the experiment, the PS of the formulation was less than 200 nm. The ZP was around -35 to -38 mV, highlighting the stability and uniformity of CAP nanobubbles. PdI values remained relatively consistent throughout the study at all temperatures indicated a uniform particle size distribution. Hydrogen bonding interactions were emphasized as critical factors in forming bulk nanobubbles and their exceptional long-lasting stability.[33,34] Nevertheless, the literature lacks consensus on the precise mechanisms underlying the stability of bulk nanobubbles, leaving this aspect unresolved.

Pharmacokinetic studies

Figure 9 displayed the plasma concentration-time curve after administration of CAP in 0.25% w/v sodium carboxymethylcellulose solution and the optimized CAP nanobubbles orally. Pharmacokinetic data in Table 3 revealed an improved NBs formulation which exhibited significantly higher T_{max}, C_{max} (**p<0.001), AUC_{0-24} (**p<0.001), and $AUC_{0-\infty}$ (**p<0.001) values as compared to the pure ENT suspension at

the prescribed dose. The bioanalytical chromatogram indicated drug retention time at 6.24 min and an internal standard (Carbamazepine) at 7.49 min (Figure 10). NSPs showed a 4.10-fold increase in C_{max} and a 6.30-fold increase in AUC_{0-t} as compared to the free drug.

The concentration of NBs reached a maximum level (C_{max}) of 4.474 times higher, while the Area under the Curve (AUC_{0-t}) was 7.29 times higher than the free drug. Wistar rats were subjected to *in vivo* studies, which revealed a progressive release of the drug from the nanobubble preparation with an extended T_{max}. When the data was compared to the free drug, oral bioavailability appeared a notable improvement significantly. An enhanced bioavailability was attributed to an increased circulation of the drug at the nanoscale and an improved penetration facilitated by the polymeric carrier system.[30]

CONCLUSION

This research introduced an innovative approach for improvement of the solubility of Capsaicin (CAP) nanobubbles derived from chili peppers. By conducting a thorough investigation, the study demonstrated that nanobubbles significantly enhanced the release of drugs, indicating their potential as a new and smart delivery system. Response surface methodology ensured a precise control over the size distribution, lead to an improved uniformity. Additionally, CAP nanobubbles exhibited an exceptional stability and dissolution in the gastrointestinal tract as compared to the traditional drug suspensions, suggested a longer drug half-life and increased effectiveness. These findings highlighted a promising role of PLGA nanobubbles in an ultrasound-responsive formulations for cancer therapy, offered notable benefits such as faster dissolution rates along with a sustained, targeted drug release, and improved oral bioavailability.

CONFLICT OF INTEREST

The authors declare that there is no conflict of interest.

ETHICAL APPROVAL

The animal study protocol was designed according to the Committee for Control and Supervision of Experiments on Animals (CCSEA) and was approved by the Institutional Animal Ethics Committee (IAEC) with the protocol number 1447/PO/Re/S/11/CPCSEA-84/A.

ABBREVIATIONS

CAP: Capsaicin; **PLGA:** Polylactic acid co-glycolic acid; **EE:** Encapsulation efficiency; **AUC:** Area Under Curve; **NBs:** Nanobubbles; **ZP:** Zeta potential.

SUMMARY

The study aimed to optimize PLGA nanobubbles for sustained release of capsaicin, overcoming its hydrophobic nature and limited bioavailability. Through systematic optimization using a Box-Behnken design, nanobubbles with favourable characteristics were developed, demonstrating an enhanced drug release with ultrasound. Further analyses confirmed the absence of drug-polymer interaction, and stability studies showed no significant changes over one month. *In vivo* studies in rats revealed an increased drug absorption and sustained release kinetics. Overall, the findings suggested that CAP-loaded PLGA nanobubbles can potentially improve drug kinetics and bioavailability, with implications for targeted drug delivery using ultrasonic-responsive combinations.

REFERENCES

1. Reilly CA, Yost GS. Metabolism of capsaicinoids by P450 enzymes: a review of recent findings on reaction mechanisms, bio-activation, and detoxification processes.*Drug Metab Rev*. 2006;38(4):685-706. doi:10.1080/03602530600959557
2. Govindarajan VS, Sathyanarayana MN. Capsicum--production, technology, chemistry, and quality. Part V. Impact on physiology, pharmacology, nutrition, and metabolism; structure, pungency, pain, and desensitization sequences. Crit Rev Food Sci Nutr. 1991;29(6):435-74. doi: 10.1080/10408399109527536. PMID: 2039598.
3. Caterina MJ, Julius D. The vanilloid receptor: a molecular gateway to the pain pathway. Annu Rev Neurosci. 2001;24:487-517. doi: 10.1146/annurev.neuro.24.1.487. PMID: 11283319.
4. Koneru M, Sahu BD, Mir SM, Ravuri HG, Kuncha M, Mahesh Kumar J, *et al.* Capsaicin, the pungent principle of peppers, ameliorates alcohol-induced acute liver injury in mice via modulation of matrix metalloproteinases. Can J Physiol Pharmacol. 2018;96(4):419-27. doi: 10.1139/cjpp-2017-0473. Epub 2017 Oct 20. PMID: 29053935.
5. Jin J, Yang L, Chen F, Gu N. Drug Delivery System Based on Nanobubbles. *Interdiscip. Mater.*2022;1(4): 471-94. https://doi.org/10.1002/idm2.12050.
6. Konda M, Sampathi S. QBD approach for the development of capsaicin-loaded stearic acid-grafted chitosan polymeric micelles. *Int. J. Appl. Pharm.*2023;15(4): 131-42. https://doi.org/10.22159/ijap.2023v15i4.48101.
7. Foudas A W, Kosheleva R I, Favvas E P, Kostoglou M, Mitropoulos A C, Kyzas G Z. Fundamentals and Applications of Nanobubbles: A Review. *Chemical Engineering Research and Design*. Elsevier January 1, 2023, pp 64-86. https://doi.org/10.1016/j.cherd.2022.11.013.
8. Khan MS, Hwang J, Lee K, *et al.* Surface Composition and Preparation Method for Oxygen Nanobubbles for Drug Delivery and Ultrasound Imaging Applications.*Nanomaterials (Basel)*. 2019;9(1):48. Published 2019 Jan 2. doi:10.3390/nano9010048
9. Xu JS, Huang J, Qin R, Hinkle GH, Povoski SP, Martin EW, *et al.* Synthesizing and binding dual-mode poly (lactic-co-glycolic acid) (PLGA) nanobubbles for cancer targeting and imaging. Biomaterials. 2010;31(7):1716-22. doi: 10.1016/j.biomaterials.2009.11.052. Epub 2009 Dec 16. PMID: 20006382.
10. Mondal R, Bobde Y, Ghosh B, Giri T K. Development and Characterization of a Phospholipid Complex for Effective Delivery of Capsaicin. *Indian J. Pharm. Sci.*2019;81(6): 1011-9. https://doi.org/10.36468/pharmaceutical-sciences.598.
11. Gao J, Liu J, Meng Z, Li Y, Hong Y, Wang L, *et al.* Ultrasound-assisted C3F8-filled PLGA nanobubbles for enhanced FGF21 delivery and improved prophylactic treatment of diabetic cardiomyopathy. Acta Biomater. 2021;130:395-408. doi: 10.1016/j.actbio.2021.06.015. Epub 2021 Jun 12. PMID: 34129954.
12. Ponnaganti M Kishore Babu A. *Preparation, Characterization And Evaluation Of Chitosan Nanobubbles For The Targeted Delivery Of Ibrutinib*; 2021;8.
13. Başpınar Y, Erel-Akbaba G, Kotmakçı M, Akbaba H. Development and characterization of nanobubbles containing paclitaxel and survivin inhibitor YM155 against lung cancer. Int J Pharm. 2019;566:149-56. doi: 10.1016/j.ijpharm.2019.05.039. Epub 2019 May 23. PMID: 31129344.
14. Rangaraj N, Pailla SR, Chowta P, Sampathi S. Fabrication of Ibrutinib Nanosuspension by Quality by Design Approach: Intended for Enhanced Oral Bioavailability and Diminished Fast Fed Variability. AAPS PharmSciTech. 2019;20(8):326. doi: 10.1208/s12249-019-1524-7. PMID: 31659558.
15. Gagliardi A, Giuliano E, Venkateswararao E, *et al.* Biodegradable Polymeric Nanoparticles for Drug Delivery to Solid Tumors.*Front Pharmacol*. 2021;12:601626. Published 2021 Feb 3. doi:10.3389/fphar.2021.601626
16. Wu Y, Huang M, He C, Wang K, Nhung NTH, Lu S, *et al.* The Influence of Air Nanobubbles on Controlling the Synthesis of Calcium Carbonate Crystals. Materials

(Basel). 2022;15(21):7437. doi: 10.3390/ma15217437. PMID: 36363030; PMCID: PMC9655898.

17. Hernandez C, Abenojar EC, Hadley J, *et al.* Sink or float? Characterization of shell-stabilized bulk nanobubbles using a resonant mass measurement technique.*Nanoscale*. 2019;11(3):851-5. doi:10.1039/c8nr08763f.
18. Wang Q, Zhao H, Qi N, Qin Y, Zhang X, Li Y. Generation and Stability of Size-Adjustable Bulk Nanobubbles Based on Periodic Pressure Change.*Sci Rep*. 2019;9(1):1118. Published 2019 Feb 4. doi:10.1038/s41598-018-38066-5
19. Sahin K, Kucuk O, Orhan C, *et al.* Bioavailability of a Capsaicin Lipid Multi-particulate Formulation in Rats [published correction appears in Eur J Drug Metab Pharmacokinet. 2021 Aug 22;:].*Eur J Drug Metab Pharmacokinet*. 2021;46(5):645-50. doi:10.1007/s13318-021-00697-x.
20. Burgess MT, Porter TM. Control of Acoustic Cavitation for Efficient Sonoporation with Phase-Shift Nanoemulsions. Ultrasound Med Biol. 2019;45(3):846-58. doi: 10.1016/j.ultrasmedbio.2018.12.001. Epub 2019 Jan 11. PMID: 30638968; PMCID: PMC8859868.
21. Kripfgans OD, Fabiilli ML, Carson PL, Fowlkes JB. On the acoustic vaporization of micrometer-sized droplets. J Acoust Soc Am. 2004;116(1):272-81. doi: 10.1121/1.1755236. PMID: 15295987.
22. Kyzas GZ, Mitropoulos AC. From Bubbles to Nanobubbles. Nanomaterials (Basel). 2021;11(10):2592. doi: 10.3390/nano11102592. PMID: 34685033; PMCID: PMC8540996.
23. Yu L X, Amidon G, Khan M A, Hoag S W, Polli J, Raju G K, *et al.* Understanding Pharmaceutical Quality by Design. *AAPS Journal*. Springer, 2014, pp 771-83. https://doi.org/10.1208/s12248-014-9598-3.
24. Bandil V, Gupta J K, Goyal M K. Formulation, Optimization and Characterization of PLGA-Chitosan Nanoparticles Containing Vinorelbine Ditartrate. *Indian J Pharm Educ Res*. 2024;58(1):99-108. https://doi.org/10.5530/ijper.58.1.10.
25. Danaei M, Dehghankhold M, Ataei S, Hasanzadeh Davarani F, Javanmard R, Dokhani A, *et al.* Impact of Particle Size and Polydispersity Index on the Clinical Applications of Lipidic Nanocarrier Systems. Pharmaceutics. 2018;10(2):57. doi: 10.3390/pharmaceutics10020057. PMID: 29783687; PMCID: PMC6027495.
26. Prabhakar A, Banerjee R. Nanobubble Liposome Complexes for Diagnostic Imaging and Ultrasound-Triggered Drug Delivery in Cancers: A Theranostic Approach. ACS Omega. 2019;4(13):15567-15580. doi: 10.1021/acsomega.9b01924. PMID: 31572858; PMCID: PMC6761614.
27. Nazzal S, Khan MA. Response surface methodology for the optimization of ubiquinone self-nanoemulsified drug delivery system. AAPS PharmSciTech. 2002;3(1):E3. doi: 10.1208/pt030103. PMID: 12916956; PMCID: PMC2750250.
28. Cavalli R, Bisazza A, Trotta M, Argenziano M, Civra A, Donalisio M, *et al.* New chitosan nanobubbles for ultrasound-mediated gene delivery: preparation and *in vitro* characterization. Int J Nanomedicine. 2012;7:3309-18. doi: 10.2147/IJN.S30912. Epub 2012 Jun 29. PMID: 22802689; PMCID: PMC3396386.
29. Almeida MA, Nadal JM, Grassiolli S, Paludo KS, Zawadzki SF, Cruz L, *et al.* Enhanced gastric tolerability and improved anti-obesity effect of capsaicinoids-loaded PCL microparticles. Mater Sci Eng C Mater Biol Appl. 2014;40:345-56. doi: 10.1016/j.msec.2014.03.049. Epub 2014 Mar 30. PMID: 24857502.
30. Peng W, Jiang XY, Zhu Y, Omari-Siaw E, Deng WW, Yu JN, X *et al.* Oral delivery of capsaicin using MPEG-PCL nanoparticles. Acta Pharmacol Sin. 2015;36(1):139-48. doi: 10.1038/aps.2014.113. Epub 2014 Dec 1. PMID: 25434988; PMCID: PMC4571314.
31. Luan Y, Lajoinie G, Gelderblom E, Skachkov I, van der Steen AF, Vos HJ, *et al.* Lipid shedding from single oscillating microbubbles. Ultrasound Med Biol. 2014;40(8):1834-46. doi: 10.1016/j.ultrasmedbio.2014.02.031. Epub 2014 May 3. PMID: 24798388.
32. Bessone F, Argenziano M, Grillo G, Ferrara B, Pizzimenti S, Barrera G, *et al.* Low-dose curcuminoid-loaded in dextran nanobubbles can prevent metastatic spreading in prostate cancer cells. Nanotechnology. 2019;30(21):214004. doi: 10.1088/1361-6528/aaff96. Epub 2019 Jan 17. PMID: 30654342.
33. Michailidi ED, Bomis G, Varoutoglou A, Kyzas GZ, Mitrikas G, Mitropoulos AC, *et al.* Bulk nanobubbles: Production and investigation of their formation/stability mechanism. J Colloid Interface Sci. 2020;564:371-380. doi: 10.1016/j.jcis.2019.12.093. Epub 2019 Dec 23. PMID: 31918204.
34. Jin J, Feng Z, Yang F, Gu N. Bulk Nanobubbles Fabricated by Repeated Compression of Microbubbles. Langmuir. 2019;35(12):4238-45. doi: 10.1021/acs.langmuir.8b04314. Epub 2019 Mar 12. PMID: 30817886.

Cite this article: Kumar AVH, Kantlam C. Exploration of Smart Utilization of Biodegradable Nanobubbles in Intensifying the Capsaicin Bioavailability. Indian J of Pharmaceutical Education and Research. 2025;59(2s):s560-s571.